Available online at www.sciencedirect.com
ScienceDirect
Journal of the European Ceramic Society 28 (2008) 2289–2298
www.elsevier.com/locate/jeurceramsoc

Silicon nitride tools for the hot rolling of high-alloyed steel and superalloy wires – Crack growth and lifetime prediction

M. Lengauer [a,b,*], R. Danzer [a]

[a] *Institut für Struktur-und Funktionskeramik, Montanuniversität Leoben, Peter-Tunner Strasse 5, 8700 Leoben, Austria*
[b] *FH JOANNEUM GmbH, Alte Poststrasse 149, 8020 Graz, Austria*

Received 20 July 2007; received in revised form 14 February 2008; accepted 29 February 2008
Available online 24 April 2008

Abstract

For the hot rolling of wire, tools are nowadays made of cemented carbides. In service, these rollers suffer primarily from wear. Due to the properties of ceramics, improvements in tool behaviour could be expected. In a recent paper the thermal and mechanical stresses in silicon nitride rollers were analysed. In field tests – when rolling materials with high-deformation resistance – cracks developed in the ceramic rollers, which grew for a long-time period before large parts of the rollers broke apart. In more moderate conditions the rollers operated safely.

In this paper a FE model is used to analyse the in-service behaviour of cracks in the silicon nitride rollers. For the observed crack path the stress intensity factor of the cracks is determined using the weight function method. It increases up to a crack depth of around 0.35 mm and then decreases again with increasing crack depth. This explains the observed pop-in-type growth of cracks after an overload. Depending on the rolled materials, the popped in cracks have a length between approximately 0.35 and 1.2 mm. The further growth of the cracks to a length of several millimetres, which is caused by a fatigue growth mechanism, needs several thousand additional revolutions.

Keywords: Failure analysis; Fatigue; Fracture; Si_3N_4; Rolling

1. Introduction

Hot forming by rolling is a commonly used process to produce wires. Nowadays the rolling of hard materials with a high strength (e.g., high-speed steels and even superalloys) is possible.[1] The surface quality of wires made of such high-strength materials is very important, since these alloys are very notch sensitive and brittle. Therefore an inferior surface quality causes a dramatic loss of strength.

Nowadays, rollers are commonly made from cemented carbides. In general, the lifetime of the rollers is limited by wear, which causes – even in the early stages – a roughening of the roller surface in the roll groove and in consequence a loss of quality of the rolled wire.[1,2] Severe wear can even change the geometry in the roll groove. This makes a regrinding or a replacement of the rollers necessary. To improve the surface quality of the wires and to increase the lifetime of the rollers, a search for better roller materials started several years ago.

Due to their high hardness, low-friction coefficients, good chemical stability and excellent high-temperature properties the application of ceramic materials for rolling applications has been investigated in recent years.[3–14] Several benefits have been claimed to result due to the use of silicon nitride rollers for the production of thinner steel tapes,[3] better surface quality of rolled wires, or longer tool life.[5,6] But failure of rollers was also reported, when materials with a very high-deformation resistance were rolled.[8,11–14] However, at other positions in the rolling mills, were the loading is relatively moderate (e.g., for guiding rolls in the rolling mill of Boehler Edelstahl GmbH in Kapfenberg[12–14]), silicon nitride rolls are already routinely used. They have a more than 10 times greater lifetime as the rolls used before, and yield a better surface quality of the rolled wires.

In a recent paper[13] the loading of silicon nitride rollers in operation was determined by an FE analysis. When rolling superalloy wires having a temperature of around 1060 °C, in each revolution the roller surface temperature fluctuates between around 200 and 900 °C. Nevertheless, the resulting tensile components of the thermal stresses are very small (the compressive

* Corresponding author at: FH JOANNEUM GmbH, Alte Poststrasse 149, 8020 Graz, Austria. Tel.: +43 316 5453 8413; fax: +43 316 5453 8401.
E-mail address: markus.lengauer@fh-joanneum.at (M. Lengauer).

0955-2219/$ – see front matter © 2008 Elsevier Ltd. All rights reserved.
doi:10.1016/j.jeurceramsoc.2008.02.028

are not) and can be considered negligible. Significant for the roller reliability are contact stresses, which occur due to the pressure between the wire and the rollers, and which superpose with frictional stresses. When rolling hard superalloys the resulting tensile stress amplitudes can reach almost 600 MPa (around 60% of the characteristic bending strength of the material) and are, therefore, high enough to cause serious damage. More details on the used FE model, the model results and the damage occurring in the rollers will be given in the next section.

In this paper the behaviour of cracks in the roll groove of heavily loaded silicon nitride-forming rollers is analysed. Based on the FE model results described in Refs. 13 and 14 and on the fractographic evidence concerning the path of cracks in the roll groove,[13,14] the stress intensity factor of cracks is determined using the weight function method.

2. Loading analysis of silicon nitride rolls in operation

Nowadays the rollers are made from cemented carbides. In our analysis we studied rollers made from silicon nitride. Analysed are rollers which were tested in a heavily loaded stand (DB03) in the finishing line of the rolling mill of Boehler Edelstahl GmbH in Kapfenberg, and which are the most severely loaded rollers in the mill. The diameter of the rollers is 225 mm. The rollers have a 2.65 mm deep circular groove with a radius of 8 mm. The roller gap measures 0.9 mm. The rollers are used to deform a nearly circular wire (large diameter: 8.8 mm; small diameter: 8.5 mm) to an elliptical cross-section (larger diameter: 10.49 mm; smaller diameter: 6.11 mm), which causes an average equivalent (von Mises) plastic deformation of 37%. The speed of the wire is almost 10 m/s and the frequency of the rollers is about 12 revolution/s. For rolling of a typical billet of 380 kg to a wire about 1200 revolutions of the rollers are necessary. For more details see Refs. 13 and 14.

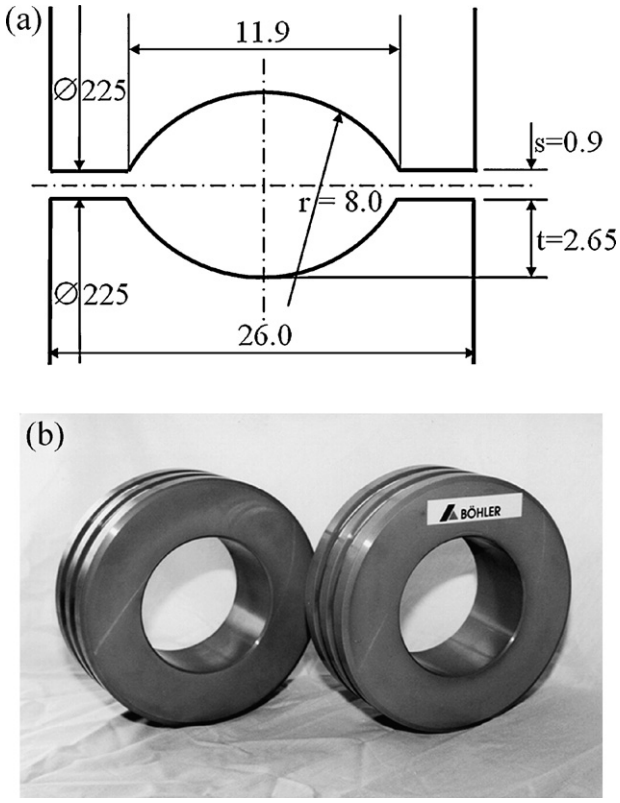

Fig. 1. Rollers at the position DB03: (a) drawing of the analysed rollers and (b) picture of a variant of the analysed rollers having two rolling grooves. The rollers (diameter 225 mm) were manufactured from silicon nitride.

A high number of different HSS steels, hot and cold-working tool steels and also nickel-base alloys are rolled with this type of roller. If not mentioned otherwise, the analysis is made for the wire material with the highest deformation resistance, i.e., for the superalloy NiCr21Mo9Nb. Its deformation resistance at the hot working temperature of 1060 °C is 725 MPa.[14,15]

The analysis is carried out with a 3D FE model. The analysed system consists of two rollers and the wire. The rotation of the rollers is modelled by applying an angular displacement to a centre node at the roller axis. To be able to describe the steep stress gradients in the rollers near the contact area with the wire a very fine grid having a width of 25 μm is used. With increasing distance from the contact area the grid width increases (up to 3 mm in the rollers and up to 1 mm in the wire). The geometry and a picture of the rollers are shown in Fig. 1. The material properties of the rollers and the wire and the other parameters used in the FE model are assumed to be independent of the temperature (which results in a small over-estimation of the stress). The Young's modulus of rollers and wire are 305 and 120 GPa, respectively, and the Poisson ratios are 0.28 and 0.33, respectively. The friction coefficient between rollers and wire is assumed to be 0.25.[16] More details concerning the used parameters (e.g., the flow curve of the wire material) and the FE model can be found in Refs. 13 and 14.

Some important model results are presented as follows. Fig. 2 shows the distribution of the first principal stress, which is pro-

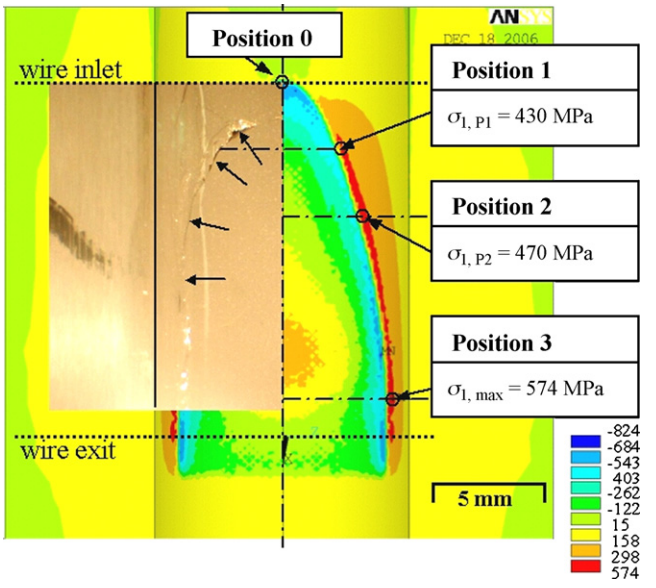

Fig. 2. Distribution of the first principal stress in the rollers: shown is a projection onto the roll groove. The insert shows a typical crack, which occurred in a field test when rolling a superalloy wire. Arrows indicate the direction of the first principal stress along the crack path.

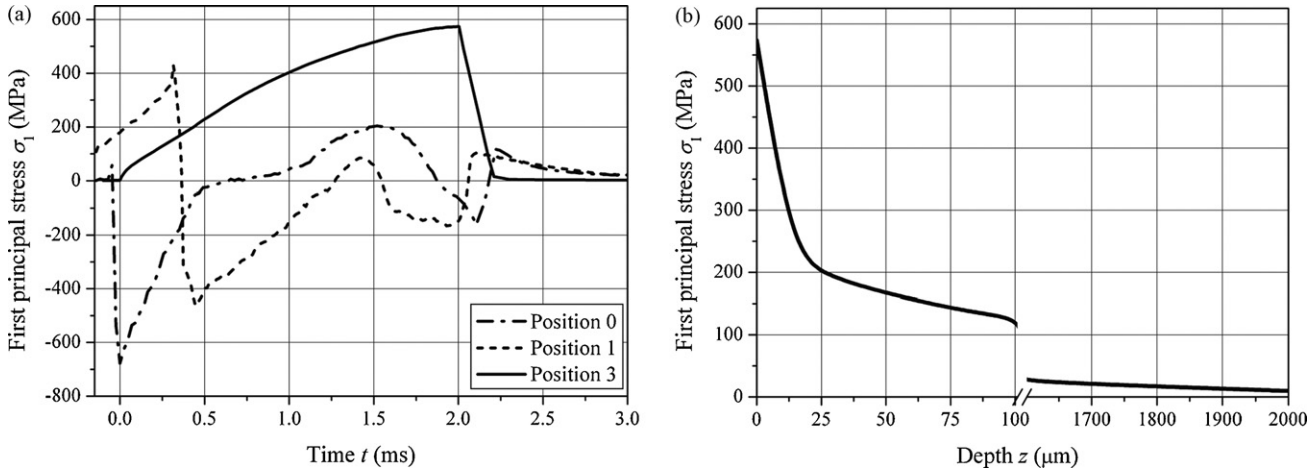

Fig. 3. Distribution of the first principal stress in the rollers: (a) course of the stress amplitude with time at the positions 0, 1, and 3 (see Fig. 2) and (b) course of the stress amplitude perpendicular to the roll groove surface starting at position 3.

jected onto the roll groove. The maximum stress amplitude occurs at position 3. It reaches 574 MPa, which is 60% of the conventionally determined bending strength (EN 843-1) of the ceramic roller material. In the contact zone[17,18] between wire and rollers the contact stresses in the ceramic are compressive. But near the edges of the contact zones significant tensile stresses occur in a near-surface region of the ceramic. In the rolling process these stresses superpose with frictional stresses, which are tensile around the centre of the contact zone and compressive ahead of and behind the contact zone. The bow-shaped zones of high-first principal stress, which exist at both sides of the roll groove, result from the superposition of these (contact and frictional) stresses as well as from the geometric relations between the roll groove and the deformed wire.[19] The insert shows a bow-shaped crack in the roll groove of a silicon nitride roller. When rolling superalloy wires, such cracks have been observed at the first inspection of the rollers after rolling a few tons of wire.[8,13,14] The occurrence and the shape of these cracks backs up the results of the FE analysis. Sometimes large pieces of roller material have broken out after this loading.

Fig. 3(a) shows the time development of the first principal stress at positions 0, 1, and 3 (see Fig. 2). In the middle of the roll groove (position 0) significant frictional stresses occur, which cause the large compressive stress at the beginning of the rolling cycle and the tensile maximum in the middle of the contact zone (after around 2.5 ms). The curve at position 3 shows a continuous increase up to the moment, where the contact zone is reached. Then the stress decreases again. At these positions friction does not contribute to the first principal stress, because of its perpendicular direction. At positions 1 and 2 a transition from the curve for position 0 to the curve for position 3 occurs and the influence of compressive stresses is significantly reduced. It should be kept in mind that the zone with the contact stresses "rotates" around the rollers.

High-stress amplitudes only occur in a very thin layer near the surface. Fig. 3(b) shows the course of the first principal stress at position 3 along a path perpendicular to the roll groove surface. Within the depth of 15 μm the stress amplitude drops to less than half. In a depth of 100 μm the stress is decreased to about one-fourth of its original amplitude.

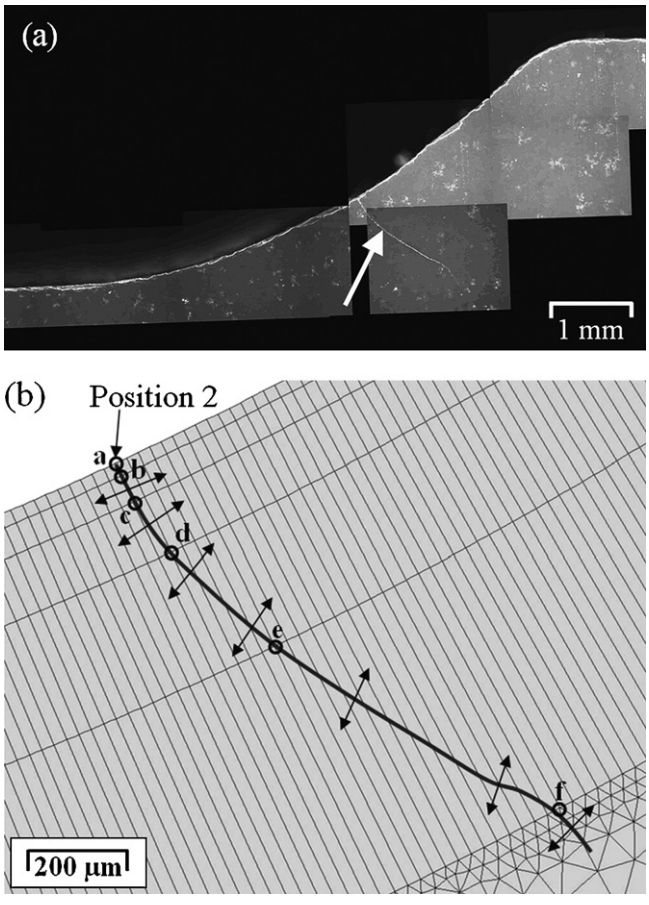

Fig. 4. (a) Polished section perpendicular to the roll groove through position 2 showing a typical crack after severe operation. (b) Magnification showing the crack path and the FE mesh. Six nodes along the path are marked with letters. Arrows indicate the direction of the first principal stress (for the time where it reaches its local maximum). It can be recognized that the crack propagation is – to a good approximation – perpendicular to the first principal stress.

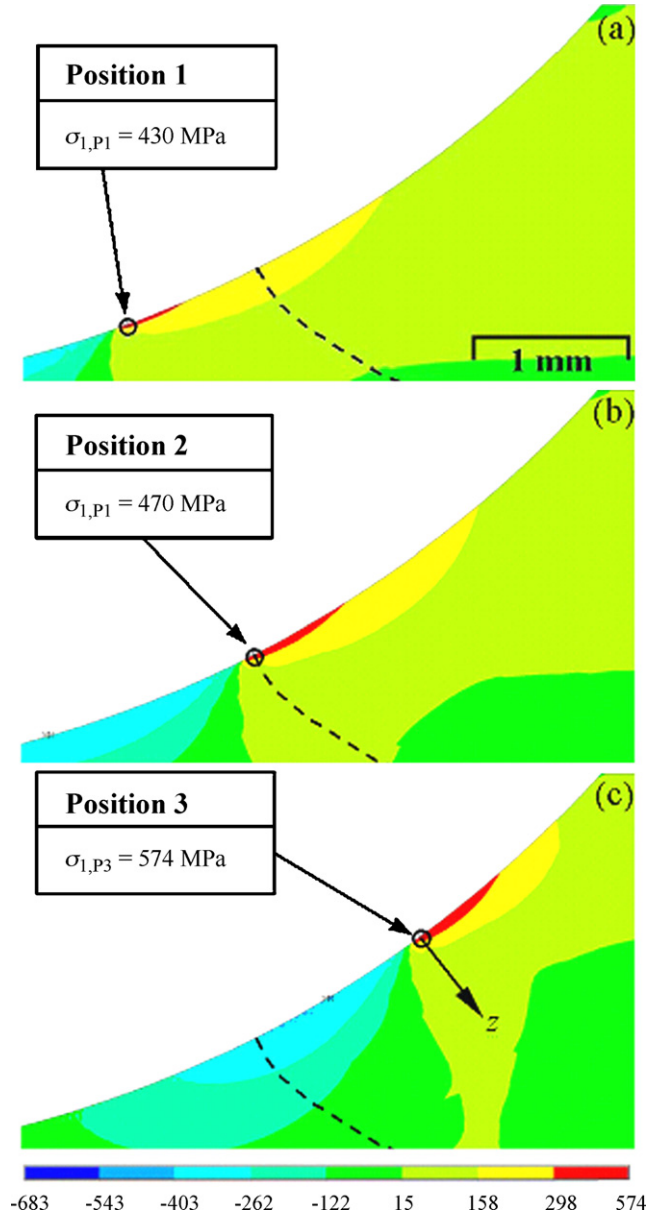

Fig. 5. Distribution of the first principal stress in the cross-section shown above after (a) 0.32 ms, (b) 0.7 ms, and (c) 2.0 ms. The dashed line marks the location of the crack shown in Fig. 4.

Field tests with silicon nitride rollers were performed at the rolling mill of Boehler Edelstahl GmbH in Kapfenberg, Austria. Results are published in Refs. 8, 11, 13, 14. The rollers could successfully be used to produce wires of soft and medium hard metals and alloys (e.g., HSS steels), but severe cracking could be observed when rolling superalloy wires. After a few tons of wire rolling (i.e., 10–20 billets, or 10^4 to 2×10^4 revolutions) the occurrence of bow-shaped cracks as shown in Fig. 2 could be observed in the roll groove. Then, circumferential cracks in the roll groove appear in the area around positions 2 and 3 (where the maximum of the tensile stress amplitude occurs), which can also cause the breaking out of large pieces of the rollers. A typical example for this type of crack is shown in Fig. 4. Several positions along the crack path are indicated with letters. The direction of the first principal stress is indicated with arrows. It is interesting to note, that the local crack path is more or less perpendicular to the direction of the local first principal stress. The deviations are smaller than 10°. In Fig. 5(a)–(c) the distribution of the first principal stress in the cross-section of the roller is shown at three different instants. Also marked is the crack path. It can be recognised that the position of the stress maximum in the cross-section moves with time from a position close to the centre of the roll groove to position 3 (see Fig. 2) at the side of the roll groove. So, the maximum tensile stress component at each position is reached at a different time, and the distribution of the local maximum of the first principal stress is given by the time envelope.[20] The course of the first principal stress at the positions marked in Fig. 4 is shown in Fig. 6(a). It can be recognised that at each position the maximum stress amplitude is reached at a different time. Fig. 6(b) shows the course of these stresses along the crack path for the times, where the stress at the positions marked in Fig. 4 is maximal. Again it can be recognised that at any position along the crack path the maximum stress is reached at a particular time, and again the distribution of local maximum of the first principal stress is given by the time envelope.

In summary, the analysis shows a complex stress field, which changes with time. It concentrates in a relatively thin layer at the surface of the roll groove around the contact zone with the wire. Due to the revolving motion of the rollers the stressed zone moves along the roll groove.

3. Stress intensity factor along the crack path

In the following the stress intensity factor of a crack of length (depth) a loaded with any traction field $\sigma(s)$ along the crack path s will be determined using the weight function method, which allows the calculation of the stress intensity factors for arbitrary loaded cracks, if – for a crack of the same geometry – the stress intensity factor is known for any special traction field (reference case)[21,22]:

$$K_{\mathrm{I}}(a) = \int_0^a \sigma(s) \cdot w(s, a)\, \mathrm{d}s. \tag{1}$$

The weight function:

$$w(s, a) = \frac{2G}{(1-\nu) \cdot K_{\mathrm{r}}(a)} \cdot \frac{\partial v_{\mathrm{r}}(s, a)}{\partial a} \tag{2}$$

depends on the reference case (stress intensity factor $K_{\mathrm{r}}(a)$, the crack opening displacement $v_{\mathrm{r}}(a)$) and on the elastic properties of the analysed material (shear modulus G, Poisson ratio ν).[21,22] The following discussion is accurate for straight cracks, but is also approximately valid for slightly curved cracks. In that sense the results are at least rough estimates. A short discussion of this point is made in Appendix A. The crack opening displacement can be determined from the traction field[23]:

$$v_{\mathrm{r}}(s, a) = \frac{1-\nu}{2G} \cdot \frac{\sigma(s)\sqrt{a}}{\sqrt{2}} \cdot \sqrt{(a-s)} \cdot \left[4f(a) + h(a) \cdot \frac{(a-s)}{a} \right], \tag{3}$$

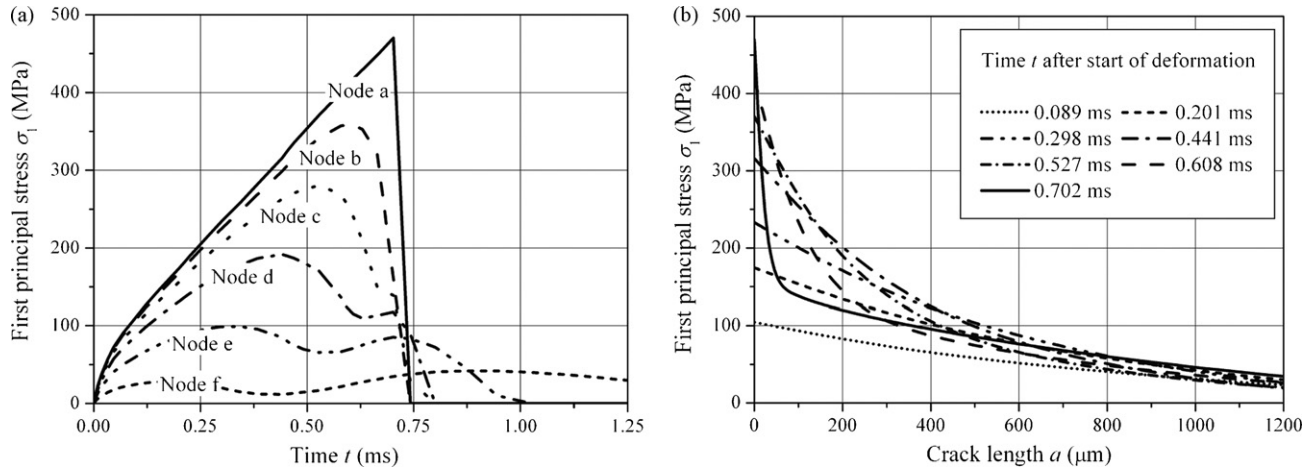

Fig. 6. (a) Course of the first principal stress at the positions (a–f) indicated in Fig. 4. (b) Course of the first principal stress along the crack path at times, where the stress reaches its maximum value at the positions marked in Fig. 4.

where $f(a)$ is the geometric factor of the reference case and the function $h(a)$ is

$$h(a) = \frac{5\pi}{\sqrt{2}a^2}\int_0^a s \cdot f^2(s)\,\mathrm{d}s - \frac{20}{3}\cdot f(a). \tag{4}$$

It is obvious that the elastic properties (G, ν) have no influence on the weight function $w(s, a)$.

tensile stress state (amplitude σ) is

$$K_\mathrm{r} = f(a)\sigma\sqrt{\pi a} = 1.12\sigma\sqrt{\pi a}, \tag{5}$$

where the geometric factor of the reference case:

$$f(a) = 1.12 \tag{6}$$

is a constant.[22] For this reference case the function $h(a)$ is also a constant: $h(a) = -0.49$. Substituting in Eqs. (1)–(3) gives the equation for the stress intensity factor:

$$K(a) = -\frac{\int_0^a \sigma(s)[1.51\sqrt{(a-s)/a} - 2.24\sqrt{a/(a-s)} + 0.25((a-s)/a)^{3/2}]\,\mathrm{d}s}{1.12\sqrt{\pi a}}. \tag{7}$$

For a circumferential crack in the roll groove an edge crack in an infinite half plane represents an adequate geometric reference model. The (reference) stress intensity factor of an edge crack in an infinite half plane loaded with a homogeneous uniaxial

The stress intensity factor of the crack in the roll groove (shown in Fig. 4) can be determined as function of time using the stress fields shown in Fig. 6(b), which describe the traction fields along the crack path at different times. For the evaluation of

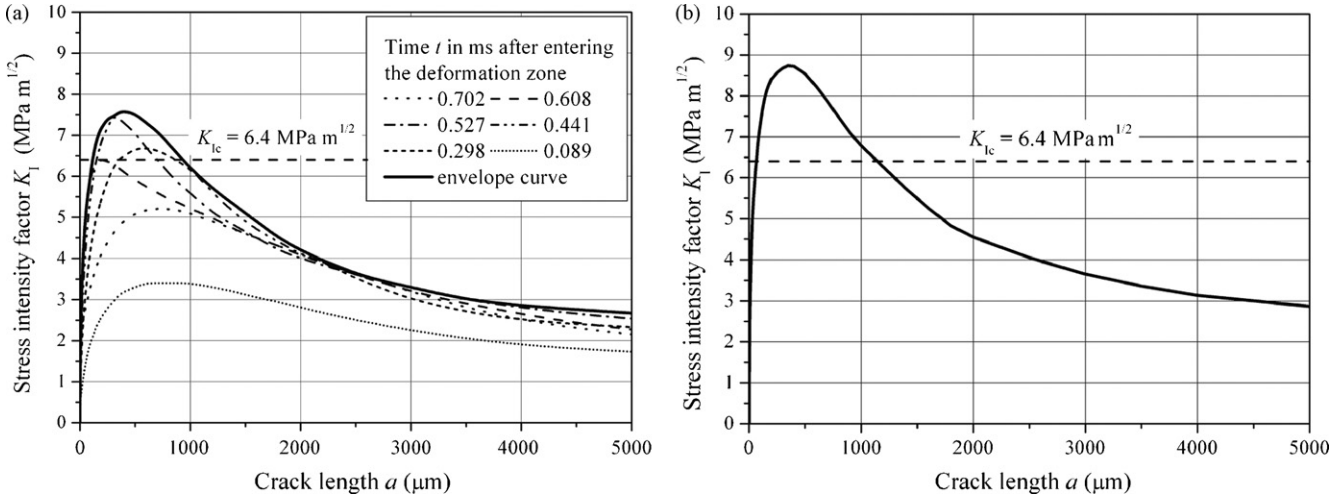

Fig. 7. Stress intensity factors of a crack in the roll groove along the crack path (a) for the crack shown in Fig. 4 (starting at position 2). Parameter in the curves is the time. The maximum loading for all positions along the crack path is given by an envelope of all curves. (b) Same envelope of the stress intensity factors at the highest loaded position in the roll groove (starting at position 3). Also indicated is the fracture toughness of the silicon nitride rollers.

Eq. (7) analytical equations were fitted to the traction fields (for more details see Ref. 14). Then the integration can easily be done using a mathematic software package, e.g., by using MAPLE. The results are plotted in Fig. 7. In part (a) the situation of the crack shown in Fig. 4 is represented. In part (b) the situation of a crack which starts at the highest loaded position in the roll groove (position 3 in Fig. 2) is shown.

It is interesting to note that the stress intensity factor has a maximum and that – depending on the time – the maximum of the stress intensity factor is positioned at a different point along the crack path. Again the maximum loading has to be described by the time envelope. In the analysed cases the maximum of the envelope is at a crack length of about 350 μm.

4. Discussion

It is assumed that crack-like flaws exist in the roll groove. Of course, spontaneous propagation of these cracks (i.e., brittle fracture) can only occur if the maximum of the stress intensity factor K is higher than the fracture toughness of the roller material. In the loading situation analysed in Fig. 7 (rolling a superalloy at the highest loaded position in the line) that is the case. For the two cracks investigated, at position 2 and at the highest loaded position 3, respectively, the maximum of the stress intensity factor reaches 7.2 and 8.7 MPa $m^{1/2}$, respectively. In comparison, the fracture toughness of the used silicon nitride material is 6.4 MPa $m^{1/2}$ (determined with the SEVNB-method,[24,25] for details of fracture toughness measurement see Ref. 26).

The contact stresses between wire and rollers do not strongly depend on the roller material (at least if very stiff materials are used) and the same holds true for the maximum of the tensile stress field. Therefore, the stress intensity factor in the rollers does not strongly depend on the roller material. Safe operation of the rollers could be achieved if a tougher roller material (toughness higher than 8.7 MPa $m^{1/2}$) were to be used. Although fracture toughness values of silicon nitride ceramics above 10 MPa $m^{1/2}$ are sometimes reported in the literature,[27] the use of silicon nitride materials having a sufficiently high toughness cannot be expected to be manageable in large industrially produced components within the foreseeable future. The state of the art solution is rollers made of cemented carbides, which have a toughness of approximately 15 MPa $m^{1/2}$ or even higher. Therefore cracks in cemented carbide rollers do not grow and these rollers fail by roughening of the surface. If, on the other hand, the rollers were to be made from silicon carbide (fracture toughness around 3–4 MPa $m^{1/2}$) failure would occur within the first revolution of the rollers even when materials with a medium deformation resistance (e.g., high-speed steels) are rolled. This has also been observed in field experiments.[14]

Safe operation of the rollers could also be achieved by reduction of tensile stresses in the roll groove. This can be done in two ways: first, the stresses scale almost linearly with the mean pressure in the contact zone between wire and rollers.[13,14] Therefore a reduction of this pressure causes a reduction of the dangerous tensile stresses. This can be done by rolling exclusively softer materials (compared to the analysed superalloy), or by reducing the wire-deformation in the roll pass. In general it can be expected that sudden crack propagation in silicon nitride rollers does not occur when rolling HSS steels (they have an about 30% lower deformation resistance than superalloys) or weaker materials. This is in agreement with experimental observations. Secondly, a reduction of the (tensile) loading can be achieved by superposing a compressive stress field to the traction stresses occurring during the rolling operation. For example this can be done by clamping the rollers between two plates. An example is analysed in Ref. 13. It is shown that this roller design can reduce the tensile stresses in the roll groove by up to 200 MPa. This would reduce the maximum of the stress intensity factor by more than 40%. Such a large reduction should even make possible the rolling of superalloy wires without the occurrence of large cracks in the roll groove.

Let us now analyse the behaviour of pre-existing cracks in the roll groove. An example for such a crack is shown in Fig. 8. The most significant result of the above calculations is that the course of the stress intensity factor versus the crack length (i.e., depth) has a maximum. Cracks can behave in the ways indicated in Fig. 9. For cracks in region I the stress intensity factor is smaller than the fracture toughness and no spontaneous crack growth is possible. In the analysed cases this happens for cracks having a depth less than 131 μm (Fig. 7(a)) or less than 66 μm (Fig. 7(b)), respectively. In the middle area of the roll groove, where the tensile loading is smaller than at the sides, much deeper cracks than at the sides would be necessary to enable crack growth.

In region II the crack intensity factor is larger than the fracture toughness and the stress intensity factor is rising. Here sudden crack extension within the first revolution of the rollers will occur. But because the crack intensity factor declines with extension, if the crack exceeds a depth of about 350 μm, it will stop, because the stress intensity factor becomes smaller than the fracture toughness (the end of region III). This is called “pop-in” behaviour. Fig. 10 shows a simulation of the crack extension based on the FE model discussed in Ref. 13. It is assumed that the local and temporal maximum of the stress intensity factor triggers the crack extension and that the crack growth is perpendicular to the first principal stress. A very good agreement

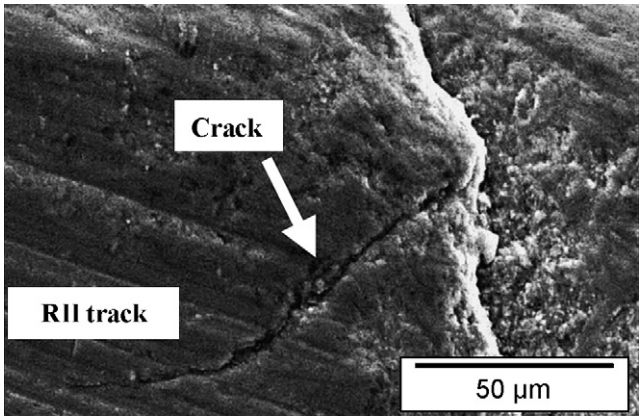

Fig. 8. Crack in the roll groove of a silicon nitride roller after machining. The roller was not in service. Severe surface damage may occur by grinding the rollers.

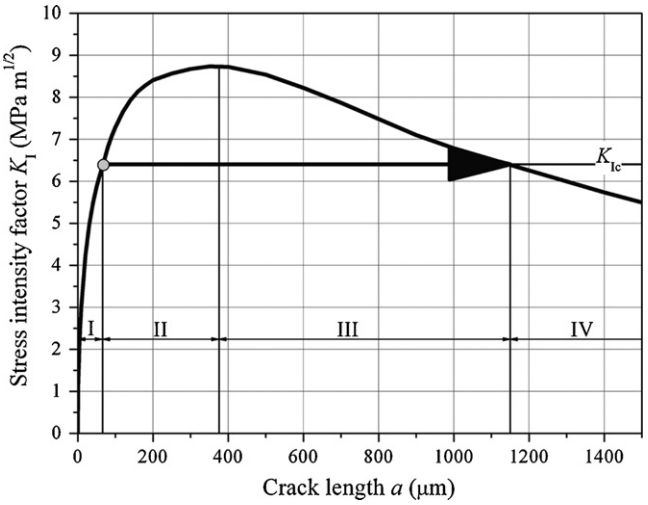

Fig. 9. Stress intensity factor of a crack starting at position 3 (where the highest loading occurs). Cracks in regions II and III will extend up to the end of region III. Cracks in regions I and IV cannot propagate spontaneously, but might do so by subcritical or cyclic fatigue crack growth processes.

between modelling and experimental results can be recognised. In fact the crack path is determined by the criterion of local symmetry, i.e., the mode II stress intensity factor vanishes at the crack tip.[28] In Appendix A it will be shown that for slightly curved cracks this criterion is, within an acceptable error margin, approximately equal to the condition that the crack follows the orthogonal field of the first principal stress.

For cracks having a depth in region III stable crack growth can occur, i.e., the cracks extend with increasing loading up to the end of region III. For the two cases shown in Fig. 7 these are lengths of about 700 and 1150 μm, respectively. In region IV the stress intensity factor is again smaller than the fracture toughness and spontaneous crack extension is not possible.

In field tests, cracks in the roll groove having a length of one to several millimetres have often been observed after rolling superalloys. Such long cracks may be caused by brittle extension of smaller cracks (as discussed above for cracks with a depth in the regions II and III). Following the above analysis this may only happen if the depth of the original cracks (before brittle extension) is between 66 μm and about 1.2 mm. In fact, ceramographic analysis of virgin rollers has shown that machining cracks, with a length of several tens of micrometers exist in the roll groove. An example is shown in Fig. 8. The existence of even larger cracks is probable. This analysis highlights the significance of a proper surface finish of the roll groove. In fact, in the field experiments, an unexpected early failure of a pair of rollers occurred after grinding of the roll groove by an inexperienced grinding shop.[14] In summary it is believed that cracks with a depth of about 66 μm or more can be caused by the machining of the roll groove. These cracks grow within the first revolution (when rolling superalloys) to a length of about 1 mm.

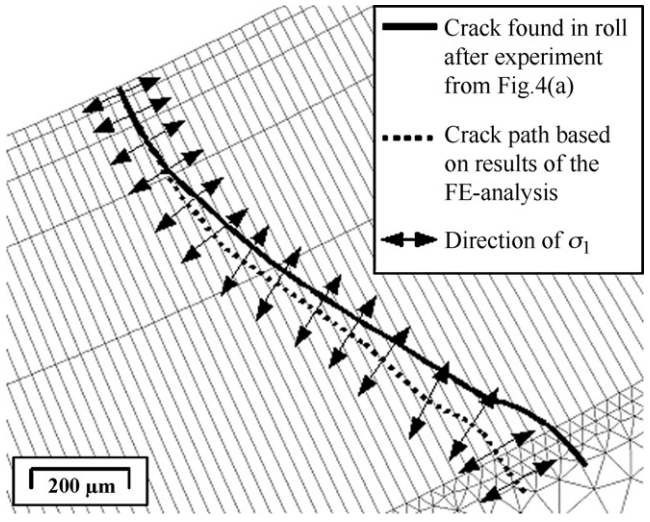

Fig. 10. Comparison of the path of a crack with the FE simulation. It is assumed that the crack grows perpendicular to the first principal stress. Also shown is the mesh of the used FE model.

Of course, further cracks can also appear in service. For example the first contact between the wire and the rollers is a kind of impact and causes a dynamic loading of the rollers. This case is not analysed in this work. It can be assumed that the impact is not very hard, because the rollers are revolving while the wire touches them and the relative velocity between wire and roller surfaces is small (about 1.5 m/s or less). If the impact causes cracking, the cracks should follow the border of the contact area, i.e., they should have a similar appearance to contact cracks (see Fig. 2). But since the first and hardest impact occurs in the middle of the roll groove, cracking should start at this position. This does not happen for the crack shown in Fig. 2, and therefore it is believed that this crack is not caused by an impact. In summary, the occurrence of impact cracks cannot be completely excluded, but seems to be unlikely to the authors. If they occur, similar behaviour to that of cracks caused by machining can be expected, and therefore the above discussion is also applicable to impact cracks. Another example for the possible occurrence of cracks in service could be the entering of hard particles (e.g., some oxidation products) into the contact area between rollers and wire. In this case these particles will be pressed into the wire. This can cause an additional local stress concentration and cracking. Again it can be expected that those cracks behave similarly to the cracks discussed above. If large hard particles get into the deformation zone, failure of the rollers may occur.

Finally, it should be discussed whether cracks in regions I and IV can grow by some kind of slow and time dependent mechanism. In the field tests, cracks with a length of more than 10 mm have been found in rollers after the rolling of some tons of superalloy wires. Sometimes these rollers were still able to operate but in other cases they failed, because large parts of the rollers broke out.[13] The existence of cracks in region IV is a clear experimental evidence that some kind of slow crack growth must have occurred. In principle, such a crack growth can occur by subcritical crack growth (a kind of stress assisted corrosion cracking) as well as by cyclic fatigue.[29,30]

Let us first discuss the subcritical crack growth mechanism.[31] In the load range $K < K_c$ the subcritical crack growth rate v can, in general, be described by a power law $v = v_0 \cdot (K/K_c)^n$, where v_0 and n are material parameters. Since the criterion of local symmetry demands, that the mode II stress intensity factor van-

ishes at the crack tip, the crack growth is triggered by the mode I stress intensity factor. The fracture toughness K_c is used as a scaling parameter.[29,31] For $K \geq K_c$ the crack growth rate is of the order of the speed of sound (sudden crack extension) and brittle fracture occurs as discussed before. An effective loading time per cycle can be defined (Δt_{eff}), which is the time under the maximum load σ_{max} within a cycle Δt, which causes the same crack advance as the real loading[30,32]:

$$\Delta t_{eff} = \int_0^{\Delta t} \left(\frac{\sigma(t)}{\sigma_{max}} \right)^n \mathrm{d}t. \quad (8)$$

At the maximal loaded position in the roll groove (position 3 in Fig. 2) the course of the stress with time is shown in Fig. 3(a). The stresses are almost zero for the majority of the loading cycle but within 2 ms they grow to the maximum. Then they fall back very quickly to zero. This part of the loading cycle can by approximated by a constant stress rate loading cycle. In this case the integral gives: $\Delta t_{eff} = \Delta t_1/(n+1)$, where Δt_1 is the time period with constant loading rate.[30] Data for subcritical crack growth in a similar silicon nitride as used for the rollers are published in Ref. 33. For cracks in region IV the temperature at the crack tip (1 mm under the surface of the roll groove) is less than 100 °C.[14] Therefore the room temperature material data can be used: $n \approx 30$ and $v_0 \approx 10^{-6}$ m/s. With $\Delta t_1 \approx 2$ ms (see Fig. 3(a)) the effective loading time per cycle is about 6×10^{-5} s. An upper limit for the subcritical crack growth rate is at $K = K_c$, where $v = v_0$. This loading occurs at the beginning of region IV. Here the crack extension due to subcritical crack growth per revolution is $\Delta a_1 \approx v_0 \cdot \Delta t_{eff} \approx 10^{-6} \cdot 6 \times 10^{-5}$ m/revolution or approximately 6×10^{-5} μm/revolution. Severe cracking of the rollers occurred within rolling of 5 tonnes of a superalloy wire, which is done in about 1.5×10^4 revolutions. In this time period crack propagation by subcritical crack growth is less than $1.5 \times 10^4 \cdot \Delta a_1 \approx 1$ μm. In other words this analysis shows that substantial subcritical crack growth does not occur for cracks in region IV. For cracks in region I the highest crack growth rate should occur at the end of region I where the stress intensity factor has its highest value and also approaches the fracture toughness: $K = K_c$. Some tens of micrometers under the surface (at the position of the crack tip) the temperature is around 700 °C.[14] Data for subcritical crack growth at this temperature are similar to those at room temperature. The subcritical crack growth rate at $K = K_c$ is again about $v_0 \approx 10^6$ m/s and the crack growth exponent n is about 30.[33] Therefore the above analysis for region IV crack is also approximately valid for cracks in region I.

Cyclic fatigue data for silicon nitride materials are reviewed in Ref. 34. Reported are data of experiments at room temperature in the tension dwell regime (this corresponds to the situation at position 3) and at a frequency of about 25 Hz. Without excessive experimental work it is not possible to assess if these data are relevant for the roller material. But the data give a rough estimation on the possible crack growth rates, which are – for the relevant range of the stress intensity factor $\Delta K = 6.4$ MPa m$^{1/2}$ – in the order of 10^{-6} m/cycle. An upper limit for the crack extension can be found by multiplying this value by the number of cycles: $1.5 \times 10^4 \cdot 10^{-6}$ m = 15 mm. It is known that fatigue crack growth may become even more severe under tension–compression loading.[29,30] Such type of loading does not occur at the highest loaded position 3 (see Fig. 2) but a little more inside the groove (e.g., at position 1 and 2, see also Fig. 3(a)). There even much larger fatigue crack propagation seems to be possible. To conclude, crack growth caused by cyclic fatigue seems to be possible for region I cracks (until the fracture toughness is reached and pop-in occurs) as well as for region IV cracks, with a significant crack advance up to several millimetres. The results of this analysis are in good agreement with the crack advance observed in experiments.

In summary, the authors believe that during the rolling of superalloys, cracks in region II instantaneously grow to lengths of about one millimetre within the first loading cycle (pop-in). Within some subsequent 10^4 cycles they grow by some kind of cyclic fatigue to a length of several millimetres. The mechanical integrity of the rollers can be guaranteed in the best way if the pop-in of the cracks at the beginning of the rolling process is avoided. Actions against this pop-in have been discussed in the above paragraphs.

5. Conclusions

In this work the behaviour of rollers at the most heavily loaded position of the end line of a rolling mill is analysed by theoretical modelling and by testing of rollers in a rolling mill at Boehler Edelstahl GmbH, Kapfenberg, Austria. The theoretical modelling can reproduce the experimental results to a large extent. It could be shown that

- Silicon nitride can be used for rollers in rolling mill finishing lines to produce wires of high-strength materials with improved surface quality.
- The life-time of the rollers is determined by the behaviour of cracks and the fracture toughness of the material.
- Cracks in the roll groove are harmless if their depth is less than about 50 μm.
- Cracks in a size interval between about 66 and 350 μm can instantaneously grow by pop-in if the fracture toughness of the roller material is too low or if the deformation resistance of the wire material is too high.
- The fracture toughness of the silicon nitride ceramic is (just) high enough to produce HSS steel wires or softer wire qualities using the conventional design. Cracks in the roll groove cannot grow by pop-in and the main damage mechanism is wear.
- The fracture toughness of the silicon nitride ceramic is too low to produce superalloy wires using the conventional roller design. Small cracks in the roll groove will pop-in to a length of about 1 mm. Then they may further grow by fatigue, which limits the lifetime of the rollers to the production of a few tonnes of superalloy wire. However a significant improvement of roller behaviour should occur and the pop-in behaviour of cracks can be prevented if additional compressive stresses are

applied across the roll groove. This can be done by clamping the rollers between two plates.

This work shows that tools for metal forming can be made from silicon nitride ceramics. Benefits are an increased tool life, a better surface quality of the product and a significant weight reduction of tools compared with the conventional solutions. In fact, silicon nitride is already routinely used at positions (e.g., guiding rolls in the rolling mill of Boehler), where wear and thermal loading is significant but the mechanical loading is less severe than in the analysed case.

Acknowledgements

Valuable comments on the behaviour of curved cracks were made by Theo Fett, Institut für Keramik im Maschinenbau, Universität Karlsruhe. Appendix A results from these comments. These contributions of Theo Fett to this paper are cordially acknowledged.

The work is partly supported by the German ministry of education and research (BMBF, 03X3503).

Appendix A. Behaviour of straight and slightly curved cracks

In Section 3 the behaviour of the crack shown in Fig. 4 is analysed. This analysis is made for a straight crack, but the crack in Fig. 4 is obviously curved. Here the situation for slightly curved cracks is shortly discussed.

For cracks under mixed mode loading mode I as well as mode II contributions of the stress intensity factor may occur in general. Results are given in Ref. 35. The criterion of local symmetry demands that in a real stress field the mode II contribution to the stress intensity factor at the crack tip disappears, i.e., the crack path is triggered by the condition $K_{II} = 0$.[28] Therefore no mixed mode failure criterion is necessary.

An analysis of the mode I stress intensity factor of slightly curved cracks under remote traction $\sigma_\infty = \text{const.}$ shows, that in a first order approximation,[36,37] the curved crack can be replaced by an edge crack normal to the surface,[38] if the angle between the tangent to the crack path and the normal to the surface is reasonable small (e.g., 30° or less). In the case analysed in Section 3, this is the case.

For oblique cracks the mode I stress intensity factor as well as the mode II stress intensity factor is a sum of terms, which are caused of principal as well as of shear components of the stress field. The details are evaluated in Ref. 39. In the actual situation the mode II contribution at the crack tip has to disappear. But since the principal and shear contributions to K_{II} due not disappear in general, this is only possible if the term arising from the principal stresses is counterbalanced from a term arising from shear stresses. Therefore the crack can not exactly follow the orthogonal of the first principal stress.[38] But in approximate analysis for slightly curved cracks[28] a first order evaluation of the mode I stress intensity factor is possible with an acceptable error margin,[28,37] i.e., if the tangent angle of the crack path to the normal of the surface is less than 15°,[38] the error is less then a few percent. For larger tangent angles the results indicate trends.

In summary the analysis made in Section 3 is a first order approximation of the behaviour of slightly curved cracks. In fact the trajectory of the crack analysed in Section 3 is orthogonal to the first principal stress field within a deviation of maximal 10°.

References

1. Dahl, W., Kopp, R. and Pawelski, O., *Umformtechnik, Plastomechanik und Werkstoffkunde*. Verlag Stahleisen, Düsseldorf, 1993.
2. Zleppnig, W., private communications, 2007.
3. Ohkohchi, T., Yasuda, K. and Nakagawa, M., Characteristics of sialon ceramic rolls in cold rolling. *ISIJ Int.*, 1992, **32**, 1250–1257.
4. BRITE EURAM Project BRPR CT-96-0343, *Large Components of Silicon Nitride Ceramics for Rolling Operations in the Steel Working Industry*, 1996.
5. Kailer, A., Kozlowski, J., Berroth, K., Wötting, G., Zleppnig, W., Danzer, R. *et al*., Keramische Walzwerkzeuge für die Herstellung von Drähten, Rohren und Bändern. *Industrie Diamanten Rundschau*, 2003, **2**, 169–172.
6. Kailer, A. and Hollstein, T., ed., *Walzen mit Keramik*. Fraunhofer IRB Verlag, Stuttgart, 2004, ISBN 3-8167-6462-2.
7. Hollstein, T., Walzen mit Keramik—Überblick über das Projekt. In *Walzen mit Keramik*, ed. A. Kailer and T. Hollstein. Fraunhofer IRB Verlag, Stuttgart, 2004, ISBN 3-8167-6462-2, pp. 7–21.
8. Lengauer, M., Danzer, R. and Harrer, W., Keramische Walzen für das Drahtwalzen—Simulation und Analyse der Werkzeugbeanspruchung. In *Walzen mit Keramik*, ed. A. Kailer and T. Hollstein. Fraunhofer IRB Verlag, Stuttgart, 2004, ISBN 3-8167-6462-2, pp. 95–108.
9. Wötting, G., Drachsler, H. and Pohlmann, H.-J., Werkstoffqualifizierung und Bauteilherstellung. In *Walzen mit Keramik*, ed. A. Kailer and T. Hollstein. Fraunhofer IRB Verlag, Stuttgart, 2004, ISBN 3-8167-6462-2, pp. 23–25.
10. Berroth, K., Herstellung und Einsatz großformatiger Walzwerkzeuge aus Siliciumnitrid. In *Walzen mit Keramik*, ed. A. Kailer and T. Hollstein. Fraunhofer IRB Verlag, Stuttgart, 2004, ISBN 3-8167-6462-2, pp. 37–47.
11. Zleppnig, W. and Keramische Drahtwalzen, Führungsrollen und Drahtführungshülsen. In *Walzen mit Keramik*, ed. A. Kailer and T. Hollstein. Fraunhofer IRB Verlag, Stuttgart, 2004, ISBN 3-8167-6462-2, pp. 85–94.
12. Lengauer, M., Danzer, R., Rubeša, D., Harrer, W. and Zleppnig, W., Failure analysis of Si_3N_4 rolls for hot wire rolling—numerical analysis of thermal and mechanical stresses. *Key Eng. Mater.*, 2004, **290**, 94–101.
13. Danzer, R., Lengauer, M., Zleppnig, W. and Harrer, W., Silicon nitride tools for hot rolling of high alloyed steel and superalloy wires—load analysis and first practical tests. *IJMR*, 2007, **11**, 1104–1114.
14. Lengauer, M., *Einsatz von Si_3N_4-Keramik als Werkstoff für Walzwerkzeuge zum Warmwalzen von Draht*. Thesis. Montanuniversität Leoben, Leoben, Austria, 2007.
15. Zhao, D., Chaudhury, P. K., Frank, R. B. and Jackman, L. A., Flow behaviour of three 625-type alloys during high temperature deformation. In *Superalloys 718, 625, 706 and Various Derivatives*, ed. E. A. Loria. The Minerals, Metals and Materials Society, Warrendale, Pennsylvania, 1994, pp. 315–329.
16. Wusatowski, Z., *Grundlagen des Walzens*. VEB Deutscher Verlag für Grundstoffindustrie, Leipzig, 1963.
17. Hertz, H., Über die Berührung fester elastischer Körper. *JRAM*, 1881, **92**, 156–171.
18. Lawn, B. R., Indentation of ceramics with spheres: a century after Hertz. *J. Am. Ceram. Soc.*, 1998, **81**, 1977–1994.
19. Johnson, K. L., *Contact Mechanics*. Cambridge University Press, 2004.
20. Danzer, R., Fischer, F. D. and Yan, W.-Y., Application of probabilistic fracture mechanics to a dynamic loading situation using the example of a dynamic tension test for ceramics. *J. Eur. Ceram. Soc.*, 2000, **20**, 901–911.
21. Betti, E., Teoria della elasticità. *Nuovo Cimento*, 1872, **2**, 6–10.
22. Gross, D., *Bruchmechanik*. Springer-Verlag, Berlin/Heidelberg, 1996.
23. Petroski, H. J. and Achenbach, J. D., Computation of the weight function from a stress intensity factor. *Eng. Fract. Mech.*, 1978, **10**, 257–266.

24. Damani, R. J., Gstrein, R. and Danzer, R., Critical notch root radius in SENB-S fracture toughness testing. *J. Eur. Ceram. Soc.*, 1996, **16**, 695–702.
25. Damani, R. J., Schuster, Ch. and Danzer, R., Polished notch modification of SENB-S fracture toughness testing. *J. Eur. Ceram. Soc.*, 1997, **17**, 1685–1689.
26. Harrer, W., Danzer, R., Lengauer, M. and Sonnleitner, M., *Drahtwalzen aus Siliciumnitrid-mechanische Eigenschaften*. Institut für Struktur-und Funktionskeramik, Montanuniversität Leoben, Leoben, 2003.
27. Petzow, G. and Herrmann, M., Silicon nitride ceramics. *Struct. Bond.*, 2002, **102**, 47–166.
28. Cotterell, B. and Rice, J. R., Some remarks on elastic crack-tip stress fields. *Int. J. Fract.*, 1980, **16**, 155–169.
29. Danzer, R., Mechanical performance and lifetime prediction. In *Concise Encyclopaedia of Advanced Ceramic Materials*, ed. R. J. Brook. Pergamon Press, Oxford, UK, 1991, pp. 286–299.
30. Munz, D. and Fett, T., *Ceramics: Mechanical Properties, Failure Behaviour, Materials Selection*. Springer-Verlag, Berlin/Heidelberg/New York, 1999.
31. Danzer, R., Sub-critical crack growth in ceramics. In *Encyclopaedia of Advanced Materials*, *vol. 4*, ed. R. W. Cahn and R. J. Brook. Pergamon Press, Oxford, UK, 1994, pp. 2693–2698.
32. Danzer, R., Lube, T., Supancic, P. and Damani, R., Fracture of ceramics. In *Ceramics Science and Technology, Vol 2*, ed. R. Riedel and I.-W. Chen. Wiley-VCH, Weinheim, Germany, in press.
33. Lube, T., Danzer, R., Kübler, J., Dusza, J., Erauw, J.-P., Klemm, H. *et al.*, Strength and fracture toughness of the ESIS silicon nitride reference material. In *Fracture Beyond 2000—Proceedings of ECF 14, Vol. II [Proceedings of ECF 14, Cracow, September 8–13, 2002, Cracow, Poland]*, 2002, pp. 409–416.
34. Gilbert, C. J., Dauskardt, R. H. and Ritchie, R. O., Microstructural mechanisms of cyclic fatigue-crack propagation in grain-bridging ceramics. *Ceram. Int.*, 1997, **23**, 413–418.
35. Fett, T. and Rizzi, G., Weight functions for stress intensity factors and T-stress for oblique cracks in a half-space. *Int. J. Fract.*, 2005, **132**, 9–16.
36. Noda, N. A. and Oda, K., Effect of curvature at the crack tip on the stress intensity factor for curved cracks. *Int. J. Fract.*, 1993, **64**, 239–249.
37. Fett, T., Rizzi, G., Bahr, H. A., Bahr, U., Pham, V. B. and Balke, H., A general weight function approach to compute mode-II stress intensity factors and crack paths for slightly curved or kinked cracks in finite bodies. *Eng. Fract. Mech.*, in press.
38. Fett, T., *Institut für Keramik im Maschinenbau*. Universität Karlsruhe (private communication), 2007.
39. Fett, T. and Munz, D., *Stress Intensity Factors and Weight Functions*. Computational Mechanics Publications, Southampton, UK, 1997.